NJC

Accepted Manuscript

This is an *Accepted Manuscript*, which has been through the Royal Society of Chemistry peer review process and has been accepted for publication.

Accepted Manuscripts are published online shortly after acceptance, before technical editing, formatting and proof reading. Using this free service, authors can make their results available to the community, in citable form, before we publish the edited article. We will replace this *Accepted Manuscript* with the edited and formatted *Advance Article* as soon as it is available.

You can find more information about *Accepted Manuscripts* in the Information for Authors.

Please note that technical editing may introduce minor changes to the text and/or graphics, which may alter content. The journal's standard Terms & Conditions and the Ethical guidelines still apply. In no event shall the Royal Society of Chemistry be held responsible for any errors or omissions in this *Accepted Manuscript* or any consequences arising from the use of any information it contains.

ROYAL SOCIETY OF CHEMISTRY

www.rsc.org/njc

One-step synthesis of porous cuprous oxide microspheres on reduced graphene oxide for selective detection of mercury ions

Shaoming Fang[1,2*], Xiaodong Dong[1], Yuanchang Zhang[1], Mengmeng Kang[1], Shunli Liu[1], Fufeng Yan[1], Linghao He[1], Xiaozhong Feng[1], Peiyuan Wang[1], Zhihong Zhang [1,2*]

E-mail addresses: mainzhh@163.com or mingfang@zzuli.edu.cn

Table of Contents (TOC)

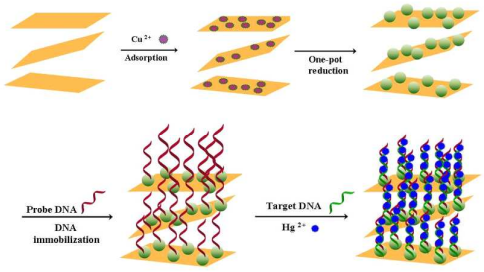

A facile one-step synthesis of Cu_2OMS-rGO nanocomposites used as sensitive layer for selective detection of mercury ions was reported.

One-step synthesis of porous cuprous oxide microspheres on reduced graphene oxide for selective detection of mercury ions

Shaoming Fang[1,2*], Xiaodong Dong[1], Yuanchang Zhang[1], Mengmeng Kang[1], Shunli Liu[1], Fufeng Yan[1], Linghao He[1], Xiaozhong Feng[1], Peiyuan Wang[1], Zhihong Zhang [1,2*]

In this paper, we report on the facile one-step synthesis of porous cuprous oxide microspheres on reduced graphene oxide (Cu_2OMS-rGO) by synchronously reducing Cu^{2+} ions and GO with ascorbic acid sodium, followed by their application as electrochemical biosensors for the detection of mercury ions in water. After detailed characterizations of the basic chemical components, crystal structure, surface morphology, and electrochemical properties of the Cu_2OMS-rGO composites, single-stranded and thymine (T)-rich oligonucleotides were successively immobilized onto the surface of the composite electrode modified by Cu_2OMS-rGO. Upon introduction of the target analyte, Hg^{2+} ions were intercalated into the DNA polyion complex membrane based on T-Hg^{2+}-T coordination chemistry. The results show that the Cu_2OMS-rGO composite has high sensitivity for the detection of Hg^{2+}, with a detection limit of 8.62 pM within the range of 0.05 nM to 40 nM. Therefore, the Cu_2OMS-rGO composite could be utilized as a novel biosensor for the detection of heavy metal ions in water or in the environment. The strategy yielded excellent selectivity of Hg^{2+} against other interfering metal ions. In addition, the developed DNA sensor for the determination of Hg^{2+} ions could be reproduced up to 10 cycles, and the recovery was approximately 95%.

1. Introduction

Some heavy metals such as lead (Pb), mercury (Hg), Arsenic (As), and cadmium (Cd) are not biologically essential and are harmful to organisms even at very low concentrations because they lead to excessive free-radical proliferation [1, 2]. Among them, mercury is a potent neurotoxin because it can accumulate in the vital organs and tissues and bind with sulfur-containing proteins and enzymes. As such, some important cell functions are inactivated, resulting in an extensive variety of diseases [3]. Therefore, to minimize heavy metal pollution, we need to develop analytical tools for heavy metal detection and prevent the damaging effects of pollution at the initial stage [4, 5]. Consequently, developing a highly sensitive and portable sensor system to detect toxic heavy metal ions is necessary. Conventional analytical techniques for heavy metals, such as atomic absorption spectrometry [6], inductively coupled plasma mass spectrometry [7], capillary electrophoresis [8], X-ray fluorescence spectrometry [9], and microprobes [10], have routinely been used for metal ion analysis with high sensitivity. Although these methods are used extensively in the laboratory and are more successful, they are unsuitable for in situ analysis because of the bulky and complication instruments. By contrast, the electrochemical technique has several advantages over these methods as it is highly sensitive, simple, fast, and inexpensive [11, 12]. Moreover, the portability and low detection limit of the electrochemical technique permit its use in online trace detection. Electrochemical impedance spectroscopy (EIS) is a technique which has been utilized by many institutions [13]. It is also an effective tool for monitoring the changes in the surface features of modified electrodes in the assembly process, and has been used to determine the adhesion of aptamer [14], protein [15], or other bimolecules [16, 17].

Evidently, electrode materials are crucial for electrochemical detection performance. Compared to the traditional electrodes materials, nanostructure materials have been the focus of considerable interest because of their enhanced electrochemical performances [4]. Electrochemical sensors using nanomaterials mainly take advantage of their large surface area, fast electronic transport properties, and high electrocatalytic activities. Many heavy metal sensors based on the use of carbon nanostructured materials [18, 19], mesoporous silica [20], and modifications using nanoparticles, such as silver [21], bismuth [22], and gold nanoparticles [23], have been reported. Among nanomaterials, cuprous oxide (Cu_2O), a p-type semiconductor with unique chemical and physical properties [24], has potential applications in electronics [25],

[1]*Henan Provincial Key Laboratory of Surface and Interface Science.* [2]*Henan Collaborative Innovation Center of Environmental Pollution Control and Ecological Resoration. Zhengzhou University of Light Industry, No. 166, Science Avenue, Zhengzhou 450001, P. R. China*
Corresponding author
Tel.: +86-37186609676 Fax: +86-37186609676
[*]E-mail addresses: mainzhh@163.com or mingfang@zzuli.edu.cn

catalysis [26], optical devices [27], and gas sensors [28]. In the past decade, various morphological Cu_2O products [29], such as hollow spheres, wires, cubes, cage and octahedron, have been synthesized by different methods. Among these products, the Cu_2O hollow sphere has been the focus of considerable attention because of its unique properties and potential application in many fields [30]. Given the high-affinity force between Cu_2O hollow spheres and DNA strands, Cu_2O hollow microspheres were used in DNA biosensor of hepatitis B virus [31].

By contrast, graphene oxide (GO), a single atomic layer of carbon arranged in a hexagonal lattice with oxygen-containing functional groups, has emerged as a novel and important class of materials due not only because of the new fundamental science but also because of the prospect of a variety of applications [32]. In particular, GO was applied as the sensitive layer in biotechnology [33]. Furthermore, the reduced form of GO (rGO) is likely to conjugate with semiconductor superstructures under the hydrothermal growth condition and consequently enhance the physical and chemical properties of the composites for diverse applications [34, 35]. It has used in havey matel ions detection [36].

In this work, we applied a one-step green synthesis of Cu_2O microspheres (Cu_2O) on the surface of rGO by synchronously reducing the Cu^{2+} ions and GO with ascorbic acid sodium. A novel and highly sensitive electrochemical biosensor based on the composities layer for detecting Hg^{2+} ion in aqueous solution was reported by our group [37]. As shown in Scheme 1, Cu^{2+} ions were adsorbed onto the surface of GO by electrostatic interaction and physical adsorption, followed by the production of Cu_2OMS-rGO composites with the presence of ascorbic acid sodium [38]. A single-stranded probe-DNA (ss-DNA) containing thymine (T) has been designed, and then immobilized on the gold surface modified by Cu_2OMS-rGO composite films. Successively, target-DNA contain T could coordinated with probe-DNA via the T-Hg^{2+}-T complex. This kind of sensor could be successfully used to detect Hg^{2+} ions with limit of detection (LOD) of 8.62 pM.

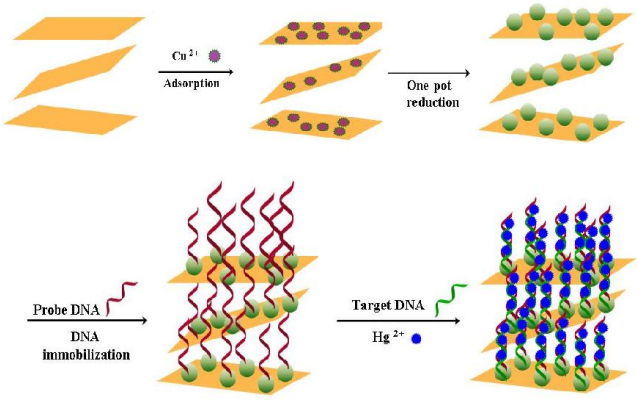

Scheme 1 Schematic of the developed immunbiosensor based on Cu_2OMS-rGO composites for detecting Hg^{2+} ions.

2. Materials and methods

2.1 Chemicals

Graphite powder (99.95%), H_2SO_4, $KMnO_4$ and H_2O_2 (30 wt%), sodium lauryl sulphate, and sodium dodecyl sulphate were obtained from Shanghai Aladdin Industrial Corporation (China). $CuSO_4·5H_2O$ and all other reagents were provided by the Sigma-Aldrich Company (St. Louis, MO, USA) and used as received. $K_3[Fe(CN)_6]$ and $K_4[Fe(CN)_6]·H_2O$ were ordered from Sinopharm Chemical Reagent Co., Ltd. (Shanghai, China). Hg^{2+} stock solution (1 mM) was prepared by dissolving $Hg(NO_3)_2$ with 0.5% HNO_3. 0.05 M Tris-HCl buffer (pH 7.4) and 0.01 M phosphate buffered saline (PBS) (pH 7.4) were prepared according to standard procedures. All solutions were prepared with Milli-Q water (≥18.2 MΩ·cm^{-1}). DNA was obtained from SBS Genetech Co. Ltd. (Beijing, China). The sequence of oligonucleotide is listed as following:

P1-DNA: 5'-GGGGGGGGGTGTTCTTCTCAGCTTTGT-3'

P2-DNA: 5'-TCTATGCTGTGTTGTACA-3'

2.2 Synthesis of Cu_2OMS-rGO composites

2.2.1 Synthesis of GO

GO was synthesized directly from graphite by using the modified Hummers method [39]. In brief, graphite (1 g) was ground with NaCl (50 g) for 10 min. NaCl was then dissolved and removed by filtration with water. The remaining graphite was stirred in 23 mL of 98% H_2SO_4 for 8 h. $KMnO_4$ (3 g) was gradually added while keeping the temperature < 20 °C. The mixture was then stirred at 80 °C for 45 min. Next, the redistilled water of 46 mL was added and the mixture was heated at 105 °C for 30 min. The reaction was terminated by addition of redistilled water (140 mL) and 30% H_2O_2 solution (10 mL). The resulting mixture was washed by repeated centrifugation and filtration, first with 5% HCl aqueous solution and then with Milli-Q water. Finally, the graphite oxide product was obtained after dried in vacuum. The exfoliation of a part of the final graphite oxide (0.5 mg/mL) to GO nanosheets was achieved by ultrasonication of the dispersion for 1 h, and then the GO aqueous dispersion was freeze-dried for further characterizations.

2.2.2 Synthesis of Cu_2O hollow nanospheres

All reagents were of analytical grade and used without further purification. In a typical procedure, 25 mL of 2 mM $CuSO_4$ solution and 0.5 g of polyvinylpyrrolidone (PVP-K30) were added into a conical flask under magnetic stirring at 25 °C. Then, 25 mL NaOH solution with pH value of 10 was added in the above mixture. After stirring for 2 min, 2.0 mL of 0.10 M $N_2H_4·H_2O$ solution was added into it. The mixed solution soon turned to be yellow. After reacting for 5 min, the product was obtained by centrifuging, washing with Milli-Q water and ethanol and then drying under vacuum at room temperature.

2.2.3 One-step synthesis of Cu_2OMS-rGO composites

The synthesis of Cu_2OMS-rGO composites was completed trough the one-step reduction process (Scheme 1). In brief, $CuSO_4·5H_2O$ (0.6 g), sodium lauryl sulfate (3.85 g) and GO (0.03

g) were mixed and dissolved with 300 mL ultrapure water. After sonication for 1 h, Cu^{2+} ions were adsorbed onto the surface of GO via electrostatic interaction and physical adsorption. Under stirring, ascorbic acid sodium (0.2 M) was added into the mixer. After 5 min, 15 mL sodium hydroxide (1M) was added into the beaker. The mixed solution was continuously stirred for 2 h until the final solution turned orange yellow. Finally, the products were centrifuged and washed with Milli-Q water for five times. Cu_2OMS-rGO composite were obtained by drying the final products at 60 °C in vacuum. 15 mg Cu_2OMS-rGO product was dispersed in 10 mL ultrapure water under ultrasonication for 5 min.

2.2.4 Preparation of phosphate buffer, DNA, and electrolyte solutions

Stock DNA solutions were prepared in PBS (pH 7.4), which was prepared by mixing 1/15 M Na_2HPO_4 and 1/15 M KH_2PO_4 in $v(Na_2HPO_4)$: $v(KH_2PO_4)$ = (8:2). The electrolyte solution was prepared immediately before use by dissolving 1.65 g of $K_3[Fe(CN)_6]$ and 2.11 g of $K_4[Fe(CN)_6]$ in 1 L of PBS.

2.2.5 Fabrication of the electrochemical biosensor based on Cu_2OMS-rGO composite for detecting Hg^{2+} ions

The gold electrode (diameter is 3 mm) was carefully cleaned before use. The electrode was immersed into fresh "piranha" solution (the mixture of 7 mL H_2SO_4 (98%) and 3 mL H_2O_2 (30%)) for 3 min, then washed with DI water and ethanol. In order to detection Hg^{2+}, 10 μL (1.5 mg/ml) of Cu_2OMS-rGO was dropped on the surface of electrode. After drying at 60℃ for 3 h, the modified electrode was immersed in 0.1 M PBS containing 200 nM P1-DNA for 8 h, and then the electrode modified with probe DNA was obtained.

2.3 Apparatus

X-ray photoelectron spectroscopy (XPS) data were collected using an AXIS HIS 165 spectrometer (Kratos Analytical, Manchester, UK) with a monochromatized Al KR X-ray source (1486.71eV photons). Field emission scanning electron microscope (FE-SEM) was collected with the JSM-6490LV scanning electron microscope (Japan). The X-ray diffraction (XRD) spectra were acquired using a D8 Advance X-ray diffraction instrument (Germany) with the scanning 2θ angle of 10° to 80°. Fourier-transform infrared (FTIR) spectra were recorded from samples in KBr pellets using a Nicolet 5700 FTIR instrument in the range of 400 to 4000cm^{-1}. Electrochemical impedance spectroscopy (EIS) and cyclic voltammetry (CV) measurements were obtained using the CHI660D electrochemical workstation (Shanghai CH Instrument Company, China).

2.4 Electrochemical measurements

All electrochemical measurements including EIS and Cyclic Voltammogram (CV) were conducted at room temperature using the CHI660D electrochemical workstation. A conventional three-electrode cell was used, which included an Ag/AgCl (saturated KCl) electrode as reference electrode, platinum slides as counter electrode, and gold eletrode as working electrode. EIS and CV were conducted in the presence of 5 mM $K_3[Fe(CN)_6]/K_4[Fe(CN)_6]$ (1:1) mixture as a redox probe in PBS (pH 7.4, containing 0.1 M KCl). The impedance spectra were collected at a potential of -0.2 V_{MSE} in the frequency range from 0.01 Hz to 100 kHz with alternating current amplitude of 5 mV. The spectra were analyzed using Zview2 software, which uses a nonlinear least-squares fit to determine the parameters of the elements in the equivalent circuit. The impedance spectra include a semicircle portion and a linear portion. The semicircle portion at high frequencies corresponds to the electron transfer process, whereas the linear portion at lower frequencies represents the diffusion process. The semicircle diameter is equal to the electron-transfer resistance (R_{ct}).

3. results and discussion

3.1 Chemical and crystal structure of graphene, Cu_2O, and Cu_2OMS-rGO composite

The chemical and crystal structure of the reduced graphene oxide, the as-prepared Cu_2O, and Cu_2OMS-rGO composites were characterized by different methods, such as Raman, XRD, FT-IR, and XPS spectroscopy, respectively **(Fig. 1)**. The Raman spectra of GO and rGO were shown in **Fig. 1a**. The D band of GO at around 1323 cm^{-1} and the G band at around 1586 cm^{-1} are clearly visible. The Raman spectrum of the rGO also contains both D and G bands (at 1323 and 1586 cm^{-1}, respectively); however, with an increased D/G intensity ratio compared to that in GO. This change suggests a decrease in the average size of the sp^2 domains upon reduction of the exfoliated GO. **Fig. 1b** shows the XRD spectra of GO, Cu_2O, and Cu_2OMS-rGO composite. The feature diffraction peak of exfoliated GO at 111 (002) is observed with interlay space (*d*-spacing) of 0.749 nm [40]. This value is larger than the *d*-spacing (0.337 nm) of pristine graphite because of the oxygenated functional groups inserted in carbon sheets [41]. For the XRD of Cu_2O, all the other peaks in the XRD pattern are indexed based on Cu_2O (JCPDS file No.: 78-2076). Four peaks with 2θ values of 31.38, 37.32, 56.35 and 68.50 correspond

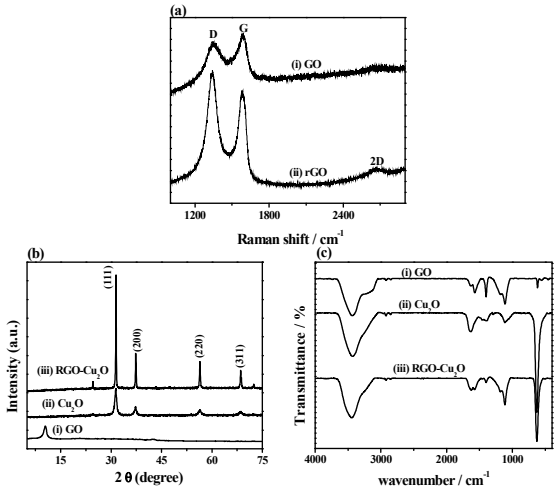

Fig. 1 (a) Raman, (b) XRD, and (c) FT-IR spectra of (i) rGO, (ii) Cu_2O, and (iii) Cu_2OMS-rGO composite.

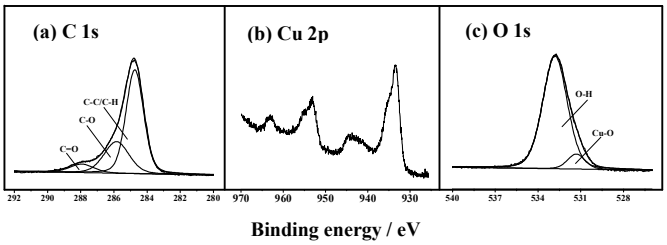

Fig. 2 (a) C 1*s*, (b) Cu 2*p*, and (c) O 1*s* core-level XPS spectra of Cu_2OMS-rGO composite.

to the (111), (200), (220) and (311) crystal planes of Cu_2O with spheres, respectively. Interestingly, diffraction peaks corresponding neither to 'CuO' nor to metallic 'Cu' are noticed. For the XRD of Cu_2OMS-rGO, four peaks similar to the peaks of Cu_2O were also observed. The peak intensity was enhanced.

The FTIR spectra of GO, Cu_2O, and Cu_2OMS-rGO composites are shown in **Fig. 1c**. The FTIR spectra of GO show aromatic C-C (1585 cm^{-1}), carboxyl O=C–O (1400 cm^{-1}), and alkoxy C–O (1110 cm^{-1}) stretching vibrational modes. The intense absorption band at 625 cm^{-1} is assigned to the copper-oxygen stretching vibration in the Cu_2O phase. By contract, the FTIR spectrum of Cu_2OMS-rGO shows three peaks at 1576 cm^{-1}, 1400 cm^{-1} and 1110 cm^{-1}, which correspond to the aromatic C-C stretch, O=C–O stretch and C–O stretch, respectively. Evidently, the characteristic absorption bands of other oxide groups decreased noticeably, indicating that GO has been reduced to rGO.

In addition, surface-sensitive XPS showed more information regarding the chemical composition of the Cu_2OMS-rGO hollow microspheres (**Fig. 2**). The peak at ~284.6 eV is assigned to C-C/C-H bond, whereas the peak at ~285.7 eV is possibly due to C-O (alcohol or ether). The peak at 287 eV is possibly due to C=O (carbonyl) in rGO (**Fig. 2a**). Peak fitting of the Cu $2p_{3/2}$ peak showed a main peak at 932.5 eV corresponding to Cu_2O and a smaller peak at the high binding energy of 934.9 eV corresponding to $Cu(OH)_2$, which could be caused by the residul of $Cu(OH)_2$ during the procedure of the preparation of Cu_2O [42]. From the O 1*s* photoelectron spectrum, the peaks located at 530.7 and 532.0 eV can be assigned to the lattice oxygen of Cu_2O and the oxygen species of surface hydroxyl groups, respectively (**Fig. 2c**).

3.2 Surface morphology of graphene, Cu_2O, and Cu_2OMS-rGO composite

The morphologies of the as-prepared GO flakes, Cu_2O hollow nanospheres, and Cu_2OMS-rGO composites were examined by FE-SEM and TEM (**Fig. 3**). The TE-SEM and TEM images of rGO clearly show the flake-like shapes with sharp edges and ripples (**Fig. 3a**). The SEM image of Cu_2O shows that the obtained particles are spheres which are made up of Cu_2O nanoparticles (Fig. 3b). The hollow feature of the nanospheres can be confirm from TEM by observing the light interior in contrast to the dark periphery, as shown in the inset of Fig. 3b. The diameter of the hollow spheres is in the range of 200 ± 20 nm

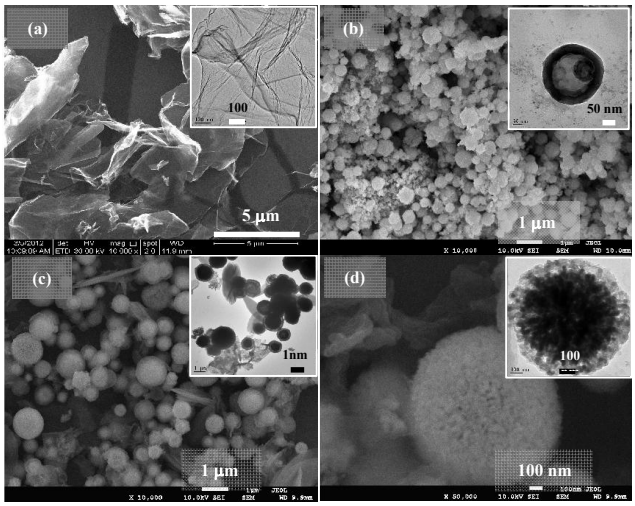

Fig. 3 Typical FE-SEM and TEM images of (a) GO, (b) Cu_2O, (c) low- magnitude, and (d) high-magnitude images of Cu_2OMS-rGO nanocomposite.

and the thickness of the hollow sphere shell is estimated to be 40 ± 5 nm for the nanosphere with a diameter of 200 nm, as shown in the inset of Fig. 3b. Fig. 3c shows the SEM image of Cu_2OMS-rGO. Compared with Cu_2O, the morphology was changed into porous nanostructures, indicating that the introduction of GO affects the nucleation and growth of Cu_2O. Alternatively, large, new and rough spheres of Cu_2OMS-rGO were formed (Figs. 3c and 3d). We also observed that the as-prepared Cu_2OMS-rGO sphere has a sea urchin-like nanostructure with an average side length of 800 ± 50 nm.

3.3 Comparison of the electrochemical performance for graphene, Cu_2O, and Cu_2OMS-rGO composite

In order to compare the eletrochemical properties of GO, Cu_2O, and Cu_2OMS-rGO composite, three nanomaterials were spin-coated on the surface of electrode following by being dried at 60 ℃ for 3 h in the vacuum oven. **Fig. 4a** shows the CVs of different electrodes coated with GO, as-prepared Cu_2O, and Cu_2OMS-rGO composite in o.1 M PBS (pH=7.4) containing 5 mM $K_3[Fe(CN)_6]$ at a scan rate of 10 mV/s. The peak to peak separation for the bare gold electrode is 0.23 V. As for the materials of Cu_2OMS-rGO, Cu_2OMS, and GO, the peak separations are 0.25 V, 0.27 V and 0.30 V, respectively. In comparison with GO and Cu_2O electrodes, the response of composite electrode modified with Cu_2OMS-rGO is obvious a pair of redox peaks corresponding to the redox of $[Fe(CN)_6]^{3-/4-}$ and shows better electrochemical performances, indicating the significant enhancement of the electron transfer rate. It also suggests that the Cu_2OMS-rGO composite can be used as the immunosensor because of its good electrochemical performance and chemically functionality.

The same result was obtained from EIS measurements, as shown in **Fig. 4b**. The simulated values of R_{ct} are 0.15, 0.45, 0.22, and 0.20 kΩ for the composite electrode of bare gold electrode, GO, Cu_2O, and Cu_2OMS-rGO composite, respectively. Moreover, the Cu_2OMS-rGO shows a relative high electrochemical

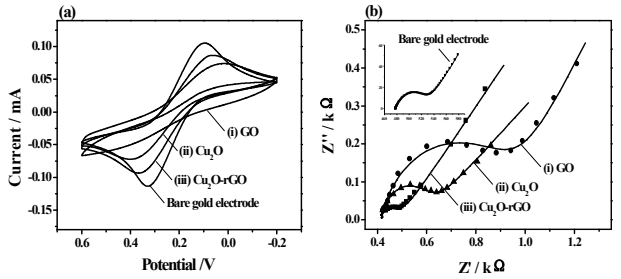

Fig. 4 (a) CV curves and (b) Nyquist plots of the electrodes containing (i) GO, (ii) as-prepared Cu_2O, and (iii) Cu_2OMS-rGO in PBS containing 5 mM $K_3[Fe(CN)_6]$ at the scan rate of 10 mV/s.

activity in comparison with GO and Cu_2O. We suggest that a synergistic effect between graphene and Cu_2O may amplify the current.

3.4 Detection of Hg^{2+} ions using the developed electrochemical biosensors based on GO, Cu_2O, and Cu_2OMS-rGO composite

Based on the electrochemical properties of the composite, the modified electrodes were immersed in 0.1 M PBS containing 100 nM DNA for 8 h. Then, the electrode modified with probe DNA was obtained. **Fig. 5** shows the EIS of the electrode at various stages for the detection of Hg^{2+} ions based on three nanomaterils, i.e., GO, Cu_2O, and Cu_2OMS-rGO. A similar trend during the processing of the composite electrode, immobilization of DNA, and the detection is observed in the three cases. After the nanomaterials were composited with the bare gold electrode, the R_{ct} value was increased, suggesting the generation of a surface with decreased conductivity on the bare gold layer. In aqueous solutions, the ss-DNA could be immobilized onto graphene, Cu_2O, and Cu_2OMS-rGO surface based on the affinity of nanomaterials and ss-DNA and their high surface area [26]. The coverage of ss-DNA on the surface inhibited the access of the electrons to the modified surface, leading to low electron transfer efficiency of the system.

The sensitive layer, such as GO, Cu_2O, and Cu_2OMS-rGO, reduced the electron transfer of the bare gold electrode, whereas the ss-DNA conversely hindered electron transfer as a shielding layer between the electrode surface and outside electrolyte solution [43, 44]. The hybridization of target DNA and coordination of Hg^{2+} ions also increased the effect of the blocking layer on the electron transfer and resulted in the continuous decrease of the electrochemical activity and increase in R_{ct}. To evaluate the efficiency of the detection of Hg^{2+} based on the different immunsensors. The simulated values of R_{ct} for each stage in the detection of Hg^{2+} for three samples areshowd in **Fig. 5d**. The differences in the R_{ct} values before and after the generation of a new layer adhesive ($\triangle R_{ct}$) could represent its relative amount [45]. Among the three samples, the addition of graphene onto the gold electrode led to the highest variation of R_{ct}, $\triangle R_{ct}$ = 0.28 kΩ. No substantial difference among $\triangle R_{ct}$ values of 0.1, 0.045, and 0.144 kΩ for GO, Cu_2O, and Cu_2OMS-rGO immunosensors, respectively, was observed after P1 immobilization. Explicitly, the variation in R_{ct} values shows a significant different once the complex of the T-Hg^{2+}-T coordination chemistry is produced. Among them, the Cu_2OMS-rGO composite shows good affinity for the ds-DNA and results in the highest variation of R_{ct}, 0.58 kΩ, whereas only $\triangle R_{ct}$ = 0.04 kΩ was calculated in the case of Cu_2O-based electrochemical immunosensor. The graphene-based system was in the intermediate between Cu_2O and Cu_2OMS-rGO samples, resulting in $\triangle R_{ct}$ = 0.37 kΩ after the coordination of Hg^{2+} with the *ds*-DNA. Although the $\triangle R_{ct}$ value of graphene after the immobilization of the *ss*-DNA is only twice as high as that of Cu_2O, its $\triangle R_{ct}$ values are approximately 10 times as high as that of Cu_2O immunosensor after the formation of the T-Hg^{2+}-T complex, indicating that Hg^{2+} could be adsorbed directly onto the network of the graphene. Explicitly, the production of the porous structure of Cu_2OMS-rGO and the synergy effect between the graphene and porous Cu_2O for bimolecular adsorption could be produced, leading to the detection of more Hg^{2+} ions.

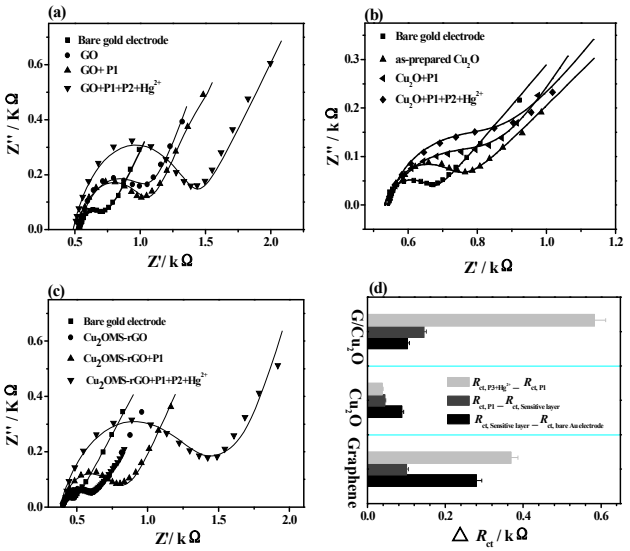

Fig. 5 Nyquist plots of EIS for 5 mM $K_3[Fe(CN)_6]/K_4[Fe(CN)_6]$ (1:1) mixture and PBS (pH 7.4, containing 0.1 M KCl) in the frequency range from 0.01 Hz to 100 kHz with 5 mV as the amplitude: bare Au electrode versus (a) GO, (b) Cu_2O, and (c) Cu_2OMS-rGO composite-modified Au electrode, P1 immobilized onto the modified Au electrode, and the coordinated electrode after reacting with P2 and 100 nM Hg^{2+}. (d) The variation in R_{ct} for the each stage in the detection of Hg^{2+} was measured using the developed immunsensors, in which GO, Cu_2O, and Cu_2OMS-rGO were used as the sensitive layers.

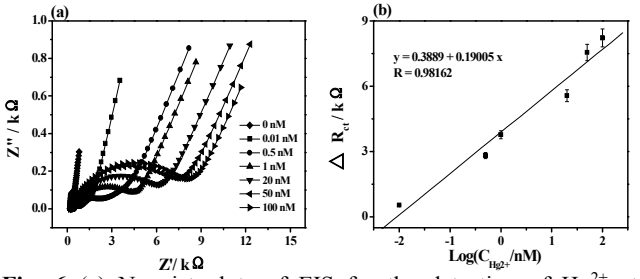

Fig. 6 (a) Nyquist plots of EIS for the detection of Hg^{2+} at different concentrations and (b) linear relationship between ΔR_{ct} and the logarithm of concentration of Hg^{2+}.

Table 1 Comparison of different Hg^{2+} detection methods

Sensitive layer	Detection technique	Linear range	LOD	Reference
AuNPs-rGO	SERS spectra	0.1 - 6,000 nM	0.1 nM	48
Gold amalgamation	Differential pulse voltammetry	0.02 - 1,000 nM	0.02 nM	49
Ag nanoclusters	Fluorescence	0.08 - 20 nM	0.08 nM	50
Aptamer along with Au-NPs	QCM	0.5 - 100 nM	0.24 nM	51
Screen-printed gold electrode	Cyclic voltammograms	10 - 10,000 nM	0.6 nM	52
Cu_2OMS-rGO	EIS	25 - 1,420 nM	8.62 pM	This work

3.5 Sensitivity of the developed immunsensor based on Cu_2OMS-rGO composite

The quantitative behavior of this assay was assessed by monitoring the dependence of the ΔR_{ct} on the amount of Hg^{2+} ions. After P1-DNA immobilization on the developed immunosensor layer, Cu_2OMS-rGO composite, Hg^{2+} with different concentrations and 100 nM P2-DNA were subsequently incubated, as shown in **Fig. 6a**. The ΔR_{ct} caused by the incubation of each mixed solution was proportional to the concentration of Hg^{2+} ions. The sensitivity of the developed DNA sensor was determined based on the values obtained for detection and quantification limits. Herein, LOD is defined as the lowest concentration of analyte that can be detected with an acceptable accuracy. LOD could be calculated from the parameters obtained from the regression curve. The linear curve fitted a regression equation of $\Delta R_{ct} = 0.3889+0.19\log C_{Hg}{}^{2+}$ with a correlation coefficient of 0.982, as shown in **Fig. 6b**. The LOD is 0.01 nM, which was estimated using three times the signal-to-noise ratio of blank solution.

In addition, the analytical performance of the developed DNA sensor for the detection of Hg^{2+} was compared with those of other Hg^{2+} assay methods reported in the literature, which are summarized in Table 1. We observed that the linear range and detection limit of the proposed DNA sensor was significantly improved, and a lower detection limit was achieved.Cu_2OMS-rGO is preferable to immobilize more DNA and to improve the electrochemical properties of the system.

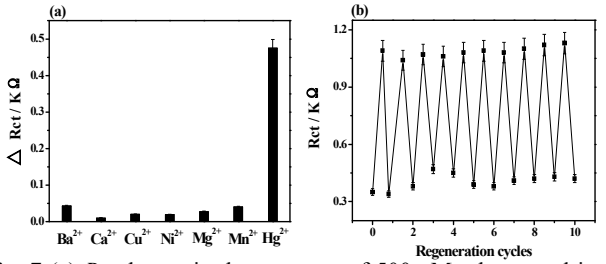

Fig. 7 (a) R_{ct} change in the presence of 500 nM other metal ions and 50 nM Hg^{2+} and (b) reusability of the EIS-based Hg^{2+} sensor challenged with 50 nM Hg^{2+} and washed with 50 mM cysteine.

3.6 Selectivity and repeatability of the developed immunsensor based on Cu_2OMS-rGO composite

The selectivity of the developed DNA sensor was studied by challenging the system against other possible interfering ions in the real sample, e.g., Co^{2+}, Cu^{2+}, Fe^{3+}, Mg^{2+}, Pb^{2+} and Zn^{2+}. As shown in **Fig. 7a**, the sensor showed significant R_{ct} increase in response to Hg^{2+}, but slightly substantial responses to other metal ions at a concentration of 500 nM, which is 50 times that of Hg^{2+}. More importantly, high-concentration interfering agents did not cause the substantial change in ΔR_{ct}. As such, the selectivity of the biosensor was acceptable. Therefore, we can conclude that this biosensor presented a satisfactory selectivity for Hg^{2+}. The chemical stability of DNA biosensor ensures that the sensor can be regenerated under proper conditions. In this work, the sensor was regenerated with 50 mM cyseine solution because of the disruption of the sandwich structure of T-Hg^{2+}-T by cysteine, as shown in **Fig. 7b**. The sensor was firstly challenged with 100 nM to obtain a response signal, followed by rinsing the cysteine solution. Afterward, the signal of the blank solution was recorded again. The procedure was repeated continuously 10 times.

3.7 Chemical component of the developed immunsensor based on Cu_2OMS-rGO composite after the detection of Hg^{2+} ions

To evaluate the chemical component of Cu_2OMS-rGO composite after being used in Hg^{2+} determination, XPS survey spectra were collected at two stages of the Cu_2OMS-rGO immobilized with P1-DNA (Cu_2OMS-rGO-P1) and Cu_2OMS-rGO with the coordinated P2-DNA and Hg^{2+} (Cu_2OMS-rGO-P1-Hg^{2+}-P2). To understand the variations in the types chemical bonds of the main elements in Cu_2OMS-rGO composite before and after the detection of Hg^{2+}, the peak-fitted C 1*s*, N 1*s*, P 2*p*, and Hg 4*f* core-level XPS spectra are summarized in **Fig. 8**. The relative content of carbon-related functional groups in the sample of Cu_2O-rGO, Cu_2O-rGO-P1, and Cu_2O-rGO-P1-Hg^{2+}-P2 were summarized in **Fig. 9**. For the C1*s* spectra of Cu_2OMS-rGO-P1 and Cu_2OMS-rGO-P1-Hg^{2+}-P2, the same fits mainly contain three component peaks, which assign to the different chemical environments present in the sample, as discussed above (Fig. 3a). However, the relative content of each functional groups were changed. This finding shows that the content of the peak at 284.6 eV decreased from 65% to 47 %, whereas the intensity of the peak at 287.5 eV (C=O or O=C-N groups) increased from 7.3% to 24 %, resulting from the presence of the oligonucleotide strands to introduce a large number of N-C=O [46].

After P1-DNA immobilization on Cu_2OMS-rGO hollow microspheres, a substantial signal of N 1*s* was observed in the sample (**Fig. 8a2** and **b2**). The same two main peaks at ~399.42 and ~400.92 eV were fitted and attributed to C-N/N-H and O=C-N groups, respectively. A new peak at low chemical shift of ~398.92 eV is obtained for the sample after the detection of Hg^{2+} (**Fig. 8b2**), which could be corresponding to N-(C=O)-N from the DNA molecule [47]. In addition, a substantial signal of P 2*p* in the sample of Cu_2OMS-rGO-P1 could be observed (**Fig. 8a3**),

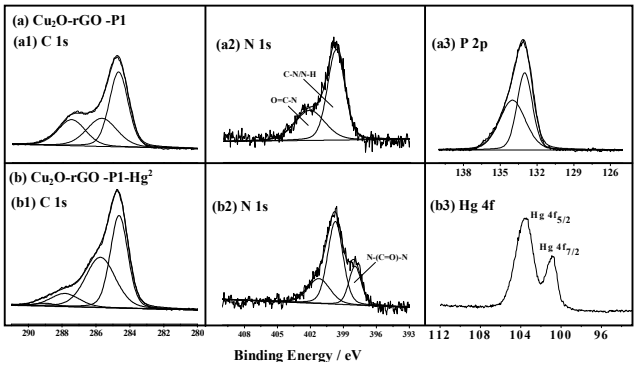

Fig. 8 C 1*s*, Cu 2*p*, N 1*s*, P 2*p*, and Hg 4*f* core-level XPS spectra of (a) Cu_2O-rGO-P1, and (b) Cu_2O-rGO-P1-Hg^{2+}-P2.

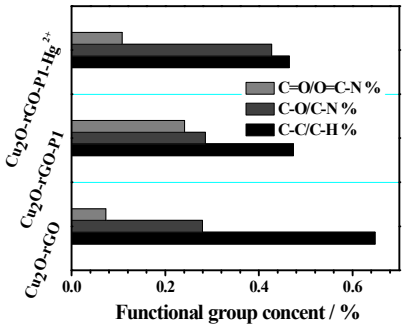

Fig. 9 The relative content of carbon-related functional groups in the sample of Cu_2O-rGO, Cu_2O-rGO-P1, and Cu_2O-rGO -P1-Hg^{2+}-P2.

indicating that the oligonucletides of P1-DNA was successfully anchored to the surface of Cu_2OMS-rGO composite. After coordinated with P2-DNA and Hg^{2+}, an apparent signal of Hg 4*f*, in which the peaks at ~100.81 and ~104.91 eV correspond to an Hg $4f_{7/2}$ and Hg $4f_{5/2}$, respectively, was observed in the final sample.

The practical application of the developed immunbiosensor for detecting Hg^{2+} ions was meausured by the determination of the recovery of spiked Hg^{2+} in river water samples. First, the water sample collected from Xushui River (Zhengzhou, China) was filtered through 0.2 μm membrances to remove impurities and then centrifugation 10 min at the speed of 8000 r/min. Subsequently, standard Hg^{2+} solutions with different concentrations were added to the pretreated water sample. The spiked samples were analyzed separately using the designed sensor. The results are shown in Table 1. And recovery values ranging from 101.1% to 104.2% were obtained, which indicated the designed sensor was applicable for Hg^{2+} analysis in real water.

Table 2 The analysis of Hg^{2+} in watersamples

Sample	Add (nmol)	Found (nmol)	Recovery (%)	RSD (%)
River water	5	5.16	103.2	3.14
	10	10.11	101.1	1.09
	80	83.37	104.2	4.12

4. Conclusions

We showed a simple and useful method for the one-step synthesis of Cu_2OMS-rGO composites. The synthesized Cu_2OMS-rGO hollow composite showed a much better electrochemical performance than that with GO and Cu_2O. Single-stranded and T-rich oligonucleitide was preferred to be immobilized onto the porous composite, followed by self-hybridization via T-Hg^{2+}-T coordination chemistry when detecting Hg^{2+} ions in water. The LOD of Hg^{2+} ions monitored through electrochemical measurements is 8.62 pM within the range of 0.05 to 40 nM. Excellent selectivity toward interfering metal ions such as Co^{2+}, Cu^{2+}, Fe^{3+}, Mg^{2+}, Pb^{2+} and Zn^{2+} can be achieved. In addition, experimental results showed that after 10 cycles, the recovery was approximately 95% for the DNA sensor in the determination of Hg^{2+} ions. Thus, the as-prepared DNA sensor based on Cu_2OMS-rGO hollow composite could be regarded as an optional scheme for the determination of Hg^{2+} and other heavy metal ions.

Acknowledgments

This work was supported by Program for the National Natural Science Foundation of China (NSFC: Account No. 51173172 and 21104070).

Author information

Corresponding author
*E-mail addresses: mainzhh@163.com
[1]Henan Provincial Key Laboratory of Surface and Interface Science,
[2]Henan Collaborative Innovation Center of Environmental Pollution Control and Ecological Resoration,
Zhengzhou University of Light Industry, No. 166, Science Avenue, Zhengzhou 450001, P. R. China.

References

1 C. Gao, X. Yu, S. Xiong, J. Liu and X. Huang. *Anal. Chem.* 2013, **85**, 2673−2680.
2 X. Yu, X. Yao, T. Luo, Y. Jia, J. Liu and X. Huang. *ACS Appl. Mater. Interfaces* 2014, **6**, 3689−3695.
3 M. Aschner and S. Walker, *Mol. Psy*. 2002, **7**, 40-S41.
4 G. Aragay, J. Pons and A. Merkoçi, *Chem. Rev.*, 2011, **111**, 3433-3458.
5 I. Bontidean, J. Ahlqvist, A. Mulchandani, W. Chen, W. Bae, R.K. Mehra, A. Mortari and E. Csöregi, *Biosen. Bioelectron.*, 2003, **18**, 547-553.
6 Z. Fang, J. Růžička and E. Hansen, *Anal. Chim. Acta.*, 1984, **164**, 23-39.
7 S. P. Dolan, D. A. Nortrup, P. M. Bolger and S. G. Caper, *J. Agr.l Food Chem.*, 2003, **51**, 1307-1312.
8 Y. Li, Y. Jiang and X. P. Yan, *Anal. Chem.*, 2006, **78**, 6115-6120.
9 O. W. Lau and S. Y. Ho, *Anal. Chim.*, 1993, **280**, 269-277.

10 A. Bernaus, X. Gaona, J. M. Esbrí, P. Higueras, G. Falkenberg and M. Valiente, *Environ. Sci. Technol.*, 2006, **40**, 4090-4095.
11 G. Aragay and A. Merkoçi, *Electrochim. Acta*, 2012, **84**, 49-61.
12 J. Herdan, R. Feeney, S. P. Kounaves and S. P. Kounaves, *Environ. Sci. Technol.*, 1998, **32**, 131-136.
13 E. P. Randviir and C. E. Banks. *Anal. Methods*, 2013, **5**, 1098-1115.
14 X. Li, L. Shen, D. Zhang, H. Qi, Q. Gao, F. Ma and C. Zhang, *Biosen. Bioelectron.*, 2008, **23**, 1624-1630.
15 A. Bogomolova, E. Komarova, K. Reber, T. Gerasimov, O. Yavuz, S. Bhatt and M. Aldissi, *Anal. Chem.*, 2009, **81**, 3944-3949.
16 H. Huang, Z. Liu, X. Yang and Anal. *Biochem.*, 2006, **356**, 208-214.
17 I. O. K'Owino, O. A and Sadik, *Electroanalysis*, 2005, **17**, 2101-2113.
18 K. Chen, G. Lu, J. Chang, S. Mao, K. H. Yu, S. Cui and J. H. Chen, *Anal. Chem.*, 2012, **84**, 4057-4062.
19 F. Arduini, C. Majorani, A. Amine, D. Moscone and G. Palleschi, *Electrochim. Acta*, 2011, **56**, 4209-4215.
20 W. Yantasee, Y. Lin, T. S. Zemanian and G. E. Fryxell, *Analyst*, 2003, **128**, 467-472.
21 Y. Wang, F. Yang and X. Yang, *ACS Appl. Mater. Inter.*, 2010, 2, 339-342.
22 E. A. Hutton, B. Ogorevc, S. B. Hočevar, F. Weldon, M. R. Smyth and J. Wang, *Electrochem. Commun.*, 2001, **3**, 707-711.
23 J. M. Gong, T. Zhou, D. Song and L. Z. Zhang, *Sensors Actuat. B*, 2010, **150**, 491-497.
24 A. Rakhshani, *Solid-State Electronics*, 1986, **29**, 7-17.
25 T. Suehiro, T. Sasaki and Y. Hiratate, *Thin solid films*, 2001, **383**, 318-320.
26 A. Sadana and J. R. Katzer, *Ind. Eng. Chem. Res.*, 1974, **13**, 127-134.
27 B. Balamurugan and B. Mehta, *Thin solid films*, 2001, **396**, 90-96.
28 X. Gou, G. Wang, J. Yang, J. Park and D. Wexler, *J. Mater. Chem.*, 2008, **18**, 965-969.
29 Q. Hua, D. Shang, W. Zhang, K. Chen, S. J. Chang, Y. S. Ma, Z. Q. Jiang and W. H. Zhang, *Langmuir*, 2010, **27**, 665-671.
30 H. Xu and W. Wang, *Angew. Chem. Int. Edi.*, 2007, **46**, 1489-1492.
31 H. Zhu, J. Wang and G. Xu, *Crystal Growth Des.*, 2008, **9**, 633-638.
32 Y. W. Zhu, S. Murali, W. W. Cai, X. S. Li, J. W. Suk, J. R. Potts and R. S. Ruoff, *Adv. Mater.*, 2010, **22**, 3906-3924.
33 Y. Wang, Z. Li, J. Wang, J. Li and Y. Lin, *Trends biotechnol.*, 2011, **29**, 205-212.
34 S. Deng, V. Tjoa, H. M. Fan, H. R. Tan, D. C. Sayle, M. Olivo, S. Mhaisalkar, J. Wei and C. H. Sow, *J. Am. Chem. Soc.*, 2012, **134**, 4905-4917.
35 S. Wu, Z. Yin, Q. He, X. Huang, X. Z. Zhou and H. Zhang, *J. Phys. Chem. C*, 2010, **114**, 11816-11821.
36 C. Gao, X. Yu, R. Xu, J. Liu and X. Huang. *ACS Appl. Mater. Interfaces* 2012, **4**, 4672−4682.
37 M. Wang, S. Liu, Y. Zhang, Y. Yang, Y. Shi, L. He, S. Fang, Z. Zhang. *Sensors and Actuators B-Chemical,* 2014, **203**, 497-503.
38 X. Mi, G. Huang, W. Xie, W. Wang, Y. Liu and J. Gao, *Carbon*, 2012, **50**, 4856-4864.
39 S. Stankovich, D. A. Dikin, R. D. Piner, K. A. Kohlhaas , A. Kleinhammes, Y. Jia, Y. Wu, S. T. Nguyen and R. S. Ruoff, *Carbon*, 2007, **45**, 1558-1565.
40 Y. J. Li, W. Gao, L. J. Ci, C. M. Wang and P. M. Ajayan, *Carbon*, 2010, **48**, 1124-1130.
41 S. Liu, J. Q. Wang, J. Zeng, J. F. Ou, Z. P. Li, X. H. Liu and S. R. Yang, *J Power Sources*, 2010, **195**, 4628-4633.
42 B. J. C. Park, J. Kim, H. Kwon and H. Song. *Adv. Mater.* 2009, **21**, 803-807.
43 Y. Xu, H. Cai, P. G. He and Y. Z. Fang, *Electroanalysis*, 2004, **16**, 150-155.
44 A. Noorbakhsh and A. Salimi, *Biosen. Bioelectron.*, 2011, **30**, 188-196.
45 A. Li, F. Yang, Y. Ma and X. R. Yang, *Biosen. Bioelectron.*, 2007, **22**, 1716-1722.
46 T. Uno, H. Tabata and T. Kawai, *Anal. Chem.*, 2007, **79**,52-59.
47 C. J. May, H. E. Canavan and D. G. Castner, *Anal. Chem.*, 2004, **76**, 1114-1122.
48 X. Ding, L. Kong, J. Wang, F. Fang, D. Li and J. Liu, *ACS Appl. Mater. Inter.*, 2013, **5**, 7072−7078.
49 J. Chen, J. Tang, J. Zhou, L. Zhang, G. Chen and D. Tang, *Anal. Chim. Acta*, 2013, **810**, 10-16.
50 J. Yin, X. He, X. Jia, K. Wang and F. Xu, *Analyst*, 2013, **138**, 2350-2356.
51 Z. M. Dong and G. C. Zhao. *Sensors*, 2012, **12**, 7080-7094.
52 X. Niu, Y. Ding, C. Chen and H. Zhao, *Sensors and Actuators B-Chemical*, 2011, **158**, 383-387.

One-step synthesis of porous cuprous oxide microspheres on reduced graphene oxide for selective detection of mercury ions

Shaoming Fang[1,2*], Xiaodong Dong[1], Yuanchang Zhang[1], Mengmeng Kang[1], Shunli Liu[1], Fufeng Yan[1], Linghao He[1], Xiaozhong Feng[1], Peiyuan Wang[1], Zhihong Zhang [1,2*]

E-mail addresses: mainzhh@163.com or mingfang@zzuli.edu.cn

Table of Contents (TOC)

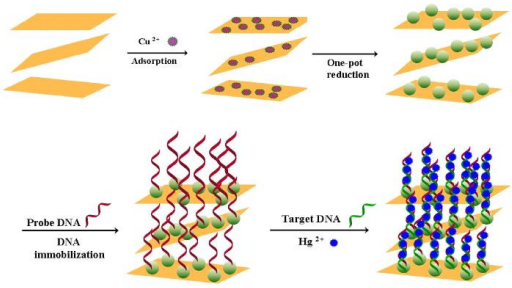

A facile one-step synthesis of Cu_2OMS-rGO nanocomposites used as sensitive layer for selective detection of mercury ions was reported.